Nonlinear Analysis: Modelling and Control, Vol. 30, No. 5, 793–810
https://doi.org/10.15388/namc.2025.30.38982

Bifurcation in a Leslie–Gower system with fear in predators and strong Allee effect in prey*

Ranchao Wu, Wenkai Xiong

School of Mathematical Sciences, Anhui University,
Hefei 230601, China
rcwu@ahu.edu.cn

Received: October 17, 2024 / **Revised:** January 27, 2025 / **Published online:** March 3, 2025

Abstract. In this paper, we consider a modified Leslie–Gower predator–prey model with Allee effect on prey and fear effect on predators. Results show complex dynamical behaviors in the model with these factors. Existence of equilibrium points and their stability of the model are first given. Then it is found that, with the Allee and fear effects, the model exhibits various and different bifurcations, such as saddle-node bifurcation, Hopf bifurcation, and Bogdanov–Takens bifurcation. Theoretical analysis is verified through some numerical simulations.

Keywords: fear effect, Allee effect, Hopf bifurcation, Bogdanov–Takens bifurcation.

1 Introduction

The predator–prey model is a fundamental ecological model that describes the interactions between two species, capturing the interaction dynamics between them and attracting persistent interests of scholars from the fields of mathematics and biology [5, 19, 21, 25, 27]. It is widely recognized that the amount of prey caught by a predator is the only factor that sustains its survival and development. In practice, however, other variables also exert an influence on predator populations. Given that the carrying capacity of the environment in a realistic situation is finite, it is reasonable to assume that the rate of increase in the number of predators is proportional to the rate of increase in the number of prey. Consequently, Leslie and Gower [12, 13] postulated that predator populations do not reproduce indefinitely in order to grow; instead, they claimed that the environmental carrying capacity of predators should be taken into consideration and proposed the modified predator–prey model known as the Leslie–Gower predator–prey model. The model proposes that the environmental carrying capacity of a predator is constrained by the size of the prey population. On the other hand, predators often prefer dietary diversity, feeding on alternative resources as favorite prey become scarce. With this in mind, Aziz-Alaou and Okiye put forth a revised Leslie–Gower model to account

*This research was supported by National Natural Science Foundation of China (No. 11971032).

for this intricacy [2]. In this case, the predator can survive even if the prey population is scarce or even extinct due to the presence of alternative prey.

In the 1930s, Allee [1] introduced the Allee effect, which states that when population densities are low, it is difficult for species to forage, find mates, fend off predators, and reproduce successfully due to environmental constraints and inbreeding leading to declining ability [6, 10, 14]. Now there are different forms of Allee effects, such as strong Allee effect [8, 24], weak Allee effect [9], multiple Allee effects [3], etc. In addition to the direct predation on prey from predators, prey frequently show some antipredator responses to the perceived predatory actions, including changes in habitats, changes in foraging behaviors, and changes in vigilance and physiology. For example, birds will flee their nests in response to antipredator defenses [7], mule deer spend less time foraging because of the threat of cougar predation [4]. This antipredator response of prey from the indirect predation is known as the fear effect. Note that the direct and indirect effects of predators are interrelated [22]. Although prey show fear effects on a regular basis, a recent experiment in [15, 18, 20] suggested that the fear effect from large carnivores may have a similar effect on medium-sized carnivores, leading to a reduction in their willingness to feed on low-nutrient organisms and causing densities of low-nutrient organisms to increase. During the experiment, a dog barking on videotape was used to simulate the fear of raccoons. Consequently, the raccoons' willingness to forage for food and the amount of time spent on eating were greatly reduced. Species at the lower level of the food chain can be effectively protected from such fear effects on predators. Therefore, it is necessary and interesting to consider fear effects on predators and the Allee effect on prey; see, for example, [13]. We will consider the modified Leslie–Gower predator–prey model with fear effect on predators and strong Allee effect on prey

$$
\begin{aligned}
\frac{\mathrm{d}x}{\mathrm{d}t} &= rx\left(1-\frac{x}{K}\right)(x-m)-\alpha xy,\\
\frac{\mathrm{d}y}{\mathrm{d}x} &= \frac{sy}{1+ky}\left(1-\frac{y}{n+\beta x}\right),
\end{aligned}
\tag{1}
$$

where x and y are the prey and predator densities at time t, respectively. The parameters r and s represent the intrinsic growth rates of the prey and predator, respectively. K is the environmental capacity of prey, m is the Allee effect threshold with $0 < m < K$, implying that it is the strong Allee effect, α denotes the conversion rate of predators, the value of k reflects the level to which fear affects the behavior of predators, β measures the quantity of prey that predators capture, n is the amount of available food that predators consume when their favourite prey is scarce or disappears from the environment [17], and all parameters are positive.

The remainder of this paper is organized into the following sections. The existence and stability of equilibrium points of system (2) are analyzed in Section 2. In Section 3, the bifurcations that occur in system (2) are described, including saddle-node bifurcation, Hopf bifurcation, and Bogdanov–Takens bifurcation. Furthermore, in Section 4, the previously derived theoretical results were verified through a series of numerical simulations. Finally, in Section 5, we provide a summary of the research presented in this paper.

2 Existence and stability of equilibria

In order to facilitate the analysis, let us simplify (1) by applying the transformation

$$x = Ku, \qquad y = K\beta v, \qquad t = \frac{kK\beta}{s}\tau$$

and still denoting u, v, and τ by x, y, and t, respectively. Then one has

$$\begin{aligned}\frac{\mathrm{d}x}{\mathrm{d}t} &= ax(1-x)(x-b) - cxy := P(x,y),\\ \frac{\mathrm{d}y}{\mathrm{d}t} &= \frac{y}{d+y}\left(1 - \frac{y}{e+x}\right) := Q(x,y),\end{aligned} \tag{2}$$

where $a = kr\beta K^2/s$, $b = m/K$, $c = \alpha k\beta^2 K^2/s$, $d = 1/(kK\beta)$, $e = n/(K\beta)$, and $0 < b < 1$. Let $P(x,y) = 0$ and $Q(x,y) = 0$, then we obtain the equilibrium $E_0 = (0,0)$, the prey-free equilibrium $E_1 = (0,e)$, and two distinct predator-free equilibria denoted as $E_2 = (b,0)$ and $E_3 = (1,0)$. With regard to the other equilibrium point (x,y) of system (2), it satisfies

$$x^2 + \left(\frac{c}{a} - b - 1\right)x + \frac{ce}{a} + b = 0. \tag{3}$$

It is evident that the equation possesses at most two equilibrium points. The following theorem is thus established.

Theorem 1. *If $b + 1 > c/a$, then*

(i) *when $e > \varDelta_0$, system* (2) *has no positive equilibrium*;

(ii) *when $e = \varDelta_0$, system* (2) *has a unique positive equilibrium*

$$E^*(x^*, y^*) = \left(\frac{ab + a - c}{2a},\ e + \frac{ab + a - c}{2a}\right);$$

(iii) *when $e < \varDelta_0$, system* (2) *has two positive equilibria*

$$\begin{aligned}E_4(x_4, y_4) &= \left(\frac{ab + a - c - a\sqrt{\varDelta}}{2a},\ e + \frac{ab + a - c - a\sqrt{\varDelta}}{2a}\right),\\ E_5(x_5, y_5) &= \left(\frac{ab + a - c + a\sqrt{\varDelta}}{2a},\ e + \frac{ab + a - c + a\sqrt{\varDelta}}{2a}\right),\end{aligned}$$

where

$$\varDelta_0 = \frac{a[(b + 1 - \frac{c}{a})^2 - 4b]}{4c}, \qquad \varDelta = \left(\frac{c}{a} - b - 1\right)^2 - 4\left(\frac{ce}{a} + b\right). \tag{4}$$

Proof. The discriminant of Eq. (3) is denoted by $\varDelta$; see (4). Obviously, if $e > \varDelta_0$, then the discriminant $\varDelta < 0$, and Eq. (3) has no solution on the real number field, i.e., there is no positive equilibrium for system (2). If $e = \varDelta_0$, then $\varDelta = 0$, and Eq. (3) possesses a unique positive solution $x^* = (ab + a - c)/(2a)$, i.e., system (2) has a unique positive equilibria $E^*((ab + a - c)(2a), e + (ab + a - c)/(2a))$. If $e < \Delta_0$, then $\Delta > 0$, and Eq. (3) has two distinct positive solutions $x_{4,5} = (ab + a - c \mp a\sqrt{\Delta})/(2a)$, i.e., system (2) exhibits two distinct positive equilibria denoted as E_4 and E_5. The proof is completed. $\square$

Theorem 2. *Equilibria E_0 and E_3 of system* (2) *are saddle-points, E_1 is a stable node, and E_2 is an unstable node.*

Proof. The Jacobian matrices of system (2) at points E_0, E_1, E_2, and E_3 are, respectively,

$$J_{E_0} = \begin{pmatrix} -ab & 0 \\ 0 & \frac{1}{d} \end{pmatrix}, \qquad J_{E_1} = \begin{pmatrix} -ab - ce & 0 \\ \frac{1}{d+e} & -\frac{1}{d+e} \end{pmatrix},$$

$$J_{E_2} = \begin{pmatrix} ab(1-b) & -bc \\ 0 & \frac{1}{d} \end{pmatrix}, \qquad J_{E_3} = \begin{pmatrix} -a(1-b) & -c \\ 0 & \frac{1}{d} \end{pmatrix}.$$

It is not difficult to find that equilibrium E_0, E_3 of system (2) are all saddle-points, E_1 is a stable node, E_2 is an unstable node. The proof is completed. $\square$

Theorem 3. *Let*

$$b + 1 > \frac{c}{a} \quad \textit{and} \quad e = \frac{a[(b + 1 - \frac{c}{a})^2 - 4b]}{4c},$$

and system (2) *has a unique positive equilibrium E^*. Then*:

(i) *if $(b-1)^2a^2 + 4acd - c^2 < 0$, equilibrium E^* is a saddle-node with a repelling parabolic sector*;

(ii) *if $(b-1)^2a^2 + 4acd - c^2 > 0$,*

   (a) *equilibrium E^* is a saddle-node with a repelling parabolic sector if $d > D_1$,*

   (b) *equilibrium E^* is a saddle-node with an attracting parabolic sector if $d < D_1$,*

where

$$D_1 = \frac{2a}{(ab + a - c)c} - \frac{a(b-1)^2}{4c} + \frac{c}{4a}.$$

Proof. The Jacobian matrix of system (2) evaluated at equilibrium E^* is

$$J_{E^*} = \begin{pmatrix} a[-3x^{*2} + (2b+2)x^* - b] - cy^* & -cx^* \\ \frac{1}{d+y^*} & -\frac{1}{d+y^*} \end{pmatrix}.$$

It readily follows that

$$\operatorname{Det}(J_{E^*}) = 0 \quad \text{and} \quad \operatorname{Tr}(J_{E^*}) = \frac{c(ab + a - c)}{2a} - \frac{4ac}{(b-1)^2a^2 + 4acd - c^2}.$$

If $(b-1)^2a^2 + 4acd - c^2 < 0$, then $\operatorname{Tr}(J_{E^*}) > 0$, so E^* is a saddle-node with a replling parabolic sector. If $(b-1)^2a^2 + 4acd - c^2 > 0$, then if $d > D_1$, we have $\operatorname{Tr}(J_{E^*}) > 0$, so E^* is a saddle-node with a repelling parabolic sector; if $d < D_1$, we have $\operatorname{Tr}(J_{E^*}) < 0$, so E^* is a saddle-node with an attracting parabolic sector. The proof is completed. $\square$

Theorem 4. *Let*

$$b+1 > \frac{c}{a} \quad \textit{and} \quad e < \frac{a[(b+1-\frac{c}{a})^2 - 4b]}{4c},$$

and system (2) *has two distinct positive equilibria E_4 and E_5. Then*:

(i) *E_4 is a saddle-node.*
(ii) *If $a[-3x_5^2 + 2(b+1)x_5 - b]a - cy_5 < 0$, then E_5 is a stable node* (*or focus*)*.*
(iii) *If $a[-3x_5^2 + 2(b+1)x_5 - b]a - cy_5 > 0$, then*
  (a) *if $d > D_2$, then E_5 is an unstable node* (*or focus*)*,*
  (b) *if $d < D_2$, then E_5 is a stable node* (*or focus*)*.*

Here

$$D_2 = \frac{1}{[-3x_5^2 + 2(b+1)x_5^2 - b]a - cy_5^2} - y_5.$$

Proof. The Jacobian matrix of system (2) evaluated at E_4 is

$$J_{E_4} = \begin{pmatrix} a[-3{x_4}^2 + (2b+2)x_4 - b] - cy_4 & -cx_4 \\ \frac{1}{d+y_4} & -\frac{1}{d+y_4} \end{pmatrix}.$$

It is clear that

$$\mathrm{Det}(J_{E_4}) = \frac{3ax_4^2 - 2a(b+1)x_4 + ab + cy_4 + cx_4}{d+y_4}.$$

Note that $d + y_4 > 0$, so the positivity of $\mathrm{Det}(J_{E_5})$ is the same as that of $3ax_4^2 - 2a(b+1)x_4 + ab + cy_4 + cx_4$. It can be obtained

$$3ax_4^2 - 2a\left[(b+1) - \frac{c}{a}\right]x_4 + ab + ce = -x_4 a\sqrt{\Delta} < 0,$$

i.e., $\mathrm{Det}(J_{E_4}) < 0$, so E_4 is a saddle-node.

Similarly, the Jacobian matrix of system (2) evaluated at E_5 is

$$J_{E_5} = \begin{pmatrix} a[-3{x_5}^2 + (2b+2)x_5 - b] - cy_5 & -cx_5 \\ \frac{1}{d+y_5} & -\frac{1}{d+y_5} \end{pmatrix},$$

then

$$\mathrm{Det}(J_{E_5}) = \frac{3ax_5^2 - 2a(b+1)x_5 + ab + cy_5 + cx_5}{d+y_5} = \frac{x_5 a\sqrt{\Delta}}{d+y_5} > 0,$$
$$\mathrm{Tr}(J_{E_5}) = a\bigl[-3x_5^2 + (2b+2)x_5 - b\bigr] - cy_5 - \frac{1}{d+y_5},$$

so the stability of E_5 is determined by the sign of $\mathrm{Tr}(J_{E_5})$. If $a[-3x_5^2 + 2(b+1) \times x_5 - b]a - cy_5 < 0$, then $\mathrm{Tr}(J_{E_5}) < 0$, and E_5 is a stable node (or focus). When $a[-3x_5^2 + 2(b+1)x_5 - b]a - cy_5 > 0$, if $d > D_2$, then $\mathrm{Tr}(J_{E_5}) > 0$, and E_5 is an unstable node (or focus); if $d < D_2$, then $\mathrm{Tr}(J_{E_5}) < 0$, and E_5 is a stable node (or focus). The proof is completed. □

3 Bifurcation analysis

Theorem 5. *When bifurcation parameter*

$$e = e_{\mathrm{SN}} = \frac{(b + 1 - \frac{c}{a})^2 a - 4ab}{4c},$$

system (2) *will experience the saddle-node bifurcation near* E^*.

Proof. The Jacobian matrix of system (2) evaluated at E^* is given by

$$J_{E^*} = \begin{pmatrix} \frac{c(ab+a-c)}{2a} & -\frac{c(ab+a-c)}{2a} \\ \frac{4ac}{(b+1)^2a^2+4acd-c^2} & -\frac{4ac}{(b+1)^2a^2+4acd-c^2} \end{pmatrix}.$$

Clearly, when $e = e_{\mathrm{SN}} = ((b+1-c/a)^2a - 4ab)/(4c)$, $\mathrm{Det}(J_{E^*}) = 0$. In this instance, the eigenvectors of matrices J_{E^*} and $J_{E^*}^{\mathrm{T}}$ are, respectively,

$$V = \begin{pmatrix} v_1 \\ v_2 \end{pmatrix} = \begin{pmatrix} 1 \\ 1 \end{pmatrix}, \qquad W = \begin{pmatrix} w_1 \\ w_2 \end{pmatrix} = \begin{pmatrix} 1 \\ -\frac{[(b-1)^2a^2+4acd-c^2](ab+a-c)}{8a^2} \end{pmatrix}.$$

Let $F(x, y) = (P(x, y), Q(x, y))^{\mathrm{T}}$, then we get

$$F_e(E^*, e_{\mathrm{SN}}) = \begin{pmatrix} 0 \\ \frac{1}{d+y^*} \end{pmatrix},$$

$$D\bigl(F_e(E^*, e_{\mathrm{SN}})\bigr)V = \begin{pmatrix} \frac{\partial P}{\partial x} & \frac{\partial P}{\partial y} \\ \frac{\partial Q}{\partial x} & \frac{\partial Q}{\partial y} \end{pmatrix} \begin{pmatrix} v_1 \\ v_2 \end{pmatrix} = \begin{pmatrix} 0 \\ -\frac{1}{d+y^*} \end{pmatrix},$$

$$D^2\bigl(F_e(E^*, e_SN)\bigr)(V, V) = \begin{pmatrix} \frac{\partial^2 P}{\partial x^2}{v_1}^2 + \frac{2\partial^2 P}{\partial x \partial y} + \frac{\partial^2 P}{\partial y^2}{v_2}^2 \\ \frac{\partial^2 Q}{\partial x^2}{v_1}^2 + \frac{2\partial^2 Q}{\partial x \partial y} + \frac{\partial^2 Q}{\partial y^2}{v_2}^2 \end{pmatrix}$$

$$= \begin{pmatrix} 2a(-3x^* + b + 1) - 2c \\ 0 \end{pmatrix}.$$

Further, we get

$$W^{\mathrm{T}} F_e(E^*, E_{\mathrm{SN}}) = \frac{w_2}{d + y^*} \neq 0, \qquad W^{\mathrm{T}}\bigl[D^2 F(E^*, E_{\mathrm{SN}})(V, V)\bigr] = 6ax^* \neq 0.$$

Therefore, system (2) will exhibit the saddle-node bifurcation at $e = e_{\mathrm{SN}}$ in view of the Sotomayor's theorem [16]. The proof is completed. □

3.1 Hopf bifurcation

From Theorem 4 the stability of E_5 changes with varying d, indicating that Hopf bifurcation may occur.

Theorem 6. *Let conditions in Theorem* 4 *are satisfied, and the stability of the positive equilibrium point* E_5 *is contingent upon the threshold value*

$$d = d_{\mathrm{H}} = \frac{1}{[-3x_5^2 + 2(b+1)x_5 - b]a - cy_5} - y_5.$$

Then the Hopf bifurcation occurs.

Proof. From the proof of Theorem 4 the characteristic equation of J_{E_5} is

$$\lambda^2 - \mathrm{Tr}(J_{E_5})\lambda + \mathrm{Det}(J_{E_5}) = 0.$$

A straightforward calculation reveals that the eigenvalues of the Jacobi matrix J_{E_5} are as follows:

$$\lambda_{1,2} = \frac{\mathrm{Tr}(J_{E_5}) \pm \sqrt{\mathrm{Tr}(J_{E_5})^2 - 4\,\mathrm{Det}(J_{E_5})}}{2}.$$

Note that

$$\frac{\mathrm{d}\,\mathrm{Tr}(J_{E_5})}{\mathrm{d}d} = \frac{1}{(d+y_5)^2} \neq 0.$$

Then the Hopf bifurcation happens at E_5 in system (2) when $d = d_{\mathrm{H}}$. As for the direction of the Hopf bifurcation, it is necessary to calculate the first Lyapunov coefficient l_1 of system (2) at E_5. Translating $E_5(x_5, y_5)$ to $(0,0)$ with $(\bar{x}, \bar{y}) = (x - x_5,\, y - y_5)$, system (2) becomes

$$\begin{aligned}
\frac{\mathrm{d}\bar{x}}{\mathrm{d}t} &= \bar{a}_{10}\bar{x} + \bar{a}_{01}\bar{y} + \bar{a}_{20}\bar{x}^2 + \bar{a}_{11}\bar{x}\bar{y} + \bar{a}_{30}\bar{x}^3 + \mathcal{O}\big(|\bar{x},\bar{y}|^4\big),\\
\frac{\mathrm{d}\bar{y}}{\mathrm{d}t} &= \bar{b}_{10}\bar{x} + \bar{b}_{01}\bar{y} + \bar{b}_{20}\bar{x}^2 + \bar{b}_{11}\bar{x}\bar{y} + \bar{b}_{02}\bar{x}^2 + \bar{b}_{30}\bar{x}^3\\
&\quad + \bar{b}_{21}\bar{x}^2\bar{y} + \bar{b}_{12}\bar{x}\bar{y}^2 + \bar{b}_{03}\bar{y}^3 + \mathcal{O}\big(|\bar{x},\bar{y}|^4\big),
\end{aligned}$$

where

$$\begin{aligned}
&\bar{a}_{10} = a\big[-3{x_5}^2 + (2b+2)x_5 - b\big] - cy_5, \qquad \bar{a}_{01} = -cx_5,\\
&\bar{a}_{20} = (-3x_5 + b + 1)a, \qquad \bar{a}_{11} = -c, \qquad \bar{a}_{30} = -a,\\
&\bar{b}_{10} = \frac{1}{d+y_5}, \qquad \bar{b}_{01} = -\frac{1}{d+y_5}, \qquad \bar{b}_{20} = -\frac{1}{(e+x_5)(d+y_5)},\\
&\bar{b}_{11} = \frac{2d+y_5}{(e+x_5)(d+y_5)^2}, \qquad \bar{b}_{02} = -\frac{d}{(e+x_5)(d+y_5)^2},\\
&\bar{b}_{30} = \frac{1}{(e+x_5)^2(d+y_5)}, \qquad \bar{b}_{21} = \frac{2d+y_5}{(e+x_5)^2(d+y_5)^2},\\
&\bar{b}_{12} = \frac{d^2}{(e+x_5)^2(d+y_5)^3}, \qquad \bar{b}_{03} = \frac{d}{(e+x_5)(d+y_5)^3}.
\end{aligned}$$

Here $\bar{a}_{10} + \bar{b}_{01} = 0$ and $\bar{a}_{10}\bar{b}_{01} - \bar{a}_{01}\bar{b}_{10} > 0$. According to [18, 23], the first Lyapunov coefficient can be given by the following formula:

$$\begin{aligned}
l_1 = \frac{-3\pi}{2\bar{a}_{01}H^{3/2}}\big\{&\big[\bar{a}_{10}\bar{b}_{10}\big(\bar{a}_{11}^2 + \bar{a}_{11}\bar{b}_{02}\big) + \bar{a}_{10}\bar{a}_{01}\big(\bar{b}_{11}^2 + \bar{a}_{20}\bar{b}_{11} + \bar{a}_{11}\bar{b}_{02}\big)\\
&- 2\bar{a}_{10}\bar{b}_{10}\bar{b}_{02}^2 - 2\bar{a}_{10}\bar{a}_{01}\big(\bar{a}_{20}^2 - \bar{b}_{20}\bar{b}_{02}\big)\\
&- \bar{a}_{10}^2(2\bar{a}_{20}\bar{b}_{20} + \bar{b}_{11}\bar{b}_{20}) + \big(\bar{a}_{01}\bar{b}_{10} - 2\bar{a}_{10}^2\big)\big(\bar{b}_{11}\bar{b}_{02} - \bar{a}_{11}\bar{a}_{20}\big)\big]\\
&- \big(\bar{a}_{10}^2 + \bar{a}_{01}\bar{b}_{10}\big)\big[3(\bar{b}_{10}\bar{b}_{03} - \bar{a}_{01}\bar{a}_{30}) + 2\bar{a}_{10}\bar{b}_{12} - \bar{a}_{10}\bar{b}_{21}\big]\big\}.
\end{aligned}$$

The Hopf bifurcation is subcritical if $l_1 > 0$, and supercritical if $l_1 < 0$. The proof is completed. □

3.2 Bogdanov–Takens bifurcation

This section will examine the Bogdanov–Takens bifurcation near E^* in detail. From Theorem 3 the Jacobian matrix at the unique positive equilibrium E^* is

$$J_{E^*} = \begin{pmatrix} a[-3x^{*2} + (2b+2)x^* - b] - cy^* & -cx^* \\ \frac{1}{d+y^*} & -\frac{1}{d+y^*} \end{pmatrix}.$$

Note that $\mathrm{Det}(J_{E^*}) = 0$ at E^*, which means that E^* is a degenerate equilibrium. Moreover, when

$$d = d_0 = \frac{2a}{c(ab + a - c)} + \frac{c}{4a} - \frac{(b-1)^2 a}{4c},$$

$\mathrm{Tr}(J_{E^*}) = 0$, then Jacobian matrix J_{E_*} has two zero characteristic roots. Then E^* is a cusp of codimension 2 by using the similar method in [26], and the Bogdanov–Takens bifurcation will occur in proximity to the value of E^*.

First, from the translation $(x_1, y_1) = (x - x^*,\ y - y^*)$ we get

$$\begin{aligned} \frac{\mathrm{d}x_1}{\mathrm{d}t} &= p_{10}x_1 + p_{01}y_1 + p_{20}x_1^2 + p_{11}x_1y_1 + \mathcal{O}\big(|x_1, y_1|^3\big), \\ \frac{\mathrm{d}y_1}{\mathrm{d}t} &= q_{10}x_1 + q_{01}y_1 + q_{20}x_1^2 + q_{11}x_1y_1 + q_{02}y_1^2 + \mathcal{O}\big(|x_1, y_1|^3\big), \end{aligned} \tag{5}$$

where

$$\begin{aligned} &p_{10} = a\big[-3x^{*2} + (2bx^* + 2)x^* - b\big] - cy^*, \qquad p_{01} = -cx^*, \\ &p_{20} = (-3x^* + b + 1)a, \qquad p_{11} = -c, \\ &q_{10} = \frac{1}{d+y^*}, \qquad q_{01} = -\frac{1}{d+y^*}, \qquad q_{20} = -\frac{1}{(e+x^*)(d+y^*)}, \\ &q_{11} = \frac{2d+y^*}{(e+x^*)(d+y^*)^2}, \qquad q_{02} = -\frac{d}{y^*(d+y^*)^2}. \end{aligned}$$

Then using the affine change $x_2 = x_1$, $y_2 = p_{10}x_1 + p_{01}y_1$, system (5) reduces to

$$\begin{aligned} \frac{\mathrm{d}x_2}{\mathrm{d}t} &= y_2 + m_{20}x_2^2 + m_{11}x_2y_2 + \mathcal{O}\big(|x_2, y_2|^3\big), \\ \frac{\mathrm{d}y_2}{\mathrm{d}t} &= n_{20}x_2^2 + n_{11}x_2y_2 + n_{02}y_2^2 + \mathcal{O}\big(|x_2, y_2|^3\big), \end{aligned} \tag{6}$$

where

$$\begin{aligned} m_{20} &= \left(p_{20} - \frac{p_{10}p_{11}}{p_0 1}\right), \qquad m_{11} = \frac{p_{11}}{p_{01}}, \qquad n_{11} = \frac{p_{10}p_{11}}{p_{01}} + q_{11} - \frac{2q_{02}p_{10}}{p_{01}}, \\ n_{20} &= p_{10}p_{20} - \frac{p_{10}^2 p_{11}}{p_{01}} + p_{01}q_{20} - q_{11}p_{10} + \frac{q_{02}p_{10}^2}{p_{01}}, \qquad n_{02} = \frac{q_{02}}{p_{01}}. \end{aligned}$$

Further applying the transformation

$$x_3 = x_2 - \frac{1}{2}(m_{11} + n_{02})x_2^2, \qquad y_3 = y_2 + m_{20}x_2^2 - n_{02}x_2y_2,$$

system (6) becomes

$$\begin{aligned}\frac{\mathrm{d}x_3}{\mathrm{d}t} &= y_3 + \mathcal{O}\big(|x_3, y_3|^3\big),\\ \frac{\mathrm{d}y_3}{\mathrm{d}t} &= \mu_1 x_3^2 + \mu_2 x_3 y_3 + \mathcal{O}\big(|x_3, y_3|^3\big),\end{aligned}$$

where $\mu_1 = n_{20}$, $\mu_2 = m_{11} + 2m_{20}$. The preceding analysis allows us to conclude that the following results can be derived.

Theorem 7. *If $\mu_1 \neq 0$, $\mu_2 \neq 0$ and $d = d_0$, then the unique positive equilibrium E^* of system* (2) *is a cusp of codimension* 2.

From the above results we know that the Bogdanov–Takens bifurcation of codimension 2 will happen at the point E^*. To further explore the bifurcation, choose c and d as the bifurcation parameters. Note that the critical values are

$$c_0 = b + 2e + 1 + 2\sqrt{be + e^2 + b + e} \quad \text{and} \quad d_0 = \frac{2a}{(ab + a - c_0)c_0} - \frac{a(b-1)^2}{4c_0} + \frac{c_0}{4a},$$

respectively. Let $c = c_0 + \lambda_1$ and $d = d_0 + \lambda_2$, where λ_1, λ_2 are the small parameters ((λ_1, λ_2) is near $(0, 0)$). Then system (2) is rewritten as

$$\begin{aligned}\frac{\mathrm{d}x}{\mathrm{d}t} &= ax(1-x)(x-b) - (c_0 + \lambda_1)xy,\\ \frac{\mathrm{d}y}{\mathrm{d}x} &= \frac{y}{d_0 + \lambda_2 + y}\left(1 - \frac{y}{e + x}\right).\end{aligned} \tag{7}$$

By the translation $z_1 = x - x^*$, $z_2 = y - y^*$, the Taylor expansion of (7) reads

$$\begin{aligned}\frac{dz_1}{\mathrm{d}t} &= a_{00}(\lambda) + a_{10}(\lambda)z_1 + a_{01}(\lambda)z_2 + a_{20}(\lambda)z_1^2 + a_{11}(\lambda)z_1z_2 + \mathcal{O}\big(|z_1, z_2|^3\big),\\ \frac{dz_2}{\mathrm{d}t} &= b_{10}(\lambda)z_1 + b_{01}(\lambda)z_2 + b_{20}(\lambda)z_1^2 + b_{11}(\lambda)z_1z_2 + b_{02}(\lambda)z_2^2 + \mathcal{O}\big(|z_1, z_2|^3\big),\end{aligned} \tag{8}$$

where λ is the vector (λ_1, λ_2), and

$$\begin{aligned}
&a_{00}(\lambda) = ax^*(1-x^*)(x^*-b) - (c_0+\lambda_1)x^*y^*, \qquad a_{01}(\lambda) = -(c_0+\lambda_1)x^*,\\
&a_{11}(\lambda) = -c_0 - \lambda_1, \qquad a_{10}(\lambda) = a\big[-3{x^*}^2 + (2b+2)x^* - b\big] - (c_0+\lambda_1)y^*,\\
&a_{20}(\lambda) = a(-3\mathrm{x}^* + \mathrm{b} + 1), \qquad b_{10}(\lambda) = \frac{1}{d_0 + \lambda_2 + y^*},\\
&b_{01}(\lambda) = -\frac{1}{d_0 + \lambda_2 + y^*}, \qquad b_{20}(\lambda) = -\frac{1}{(e+x^*)(d_0+\lambda_2+y^*)},\\
&b_{11}(\lambda) = \frac{2d_0 + 2\lambda_2 + y^*}{(e+x^*)(d_0+\lambda_2+y^*)}, \qquad b_{02}(\lambda) = -\frac{d_0+\lambda_2}{(e+x^*)(d_0+\lambda_2+y^*)^2}.
\end{aligned}$$

Here $a_{00}(0) = 0$, $a_{10}(0) + b_{01}(0) = 0$, $a_{10}(0)b_{01}(0) + a_{01}(0)b_{10}(0) = 0$. Through the affine change

$$u_1 = z_1, \qquad v_1 = a_{10}(\lambda)z_1 + a_{01}(\lambda)z_2,$$

system (8) is changed into

$$\begin{aligned} \frac{\mathrm{d}u_1}{\mathrm{d}t} &= f_{00}(\lambda) + v_1 + f_{20}(\lambda)u_1^2 + f_{11}(\lambda)u_1v_1 + \mathcal{O}(|u_1, v_1|^3), \\ \frac{\mathrm{d}v_1}{\mathrm{d}t} &= g_{00}(\lambda) + g_{10}(\lambda)u_1 + g_{01}(\lambda)v_1 + g_{20}(\lambda)u_1^2 \\ &\quad + g_{11}(\lambda)u_1v_1 + g_{02}(\lambda)v_1^2 + \mathcal{O}\big(|u_1, v_1|^3\big), \end{aligned} \tag{9}$$

where

$$\begin{aligned} &f_{00}(\lambda) = a_{00}(\lambda), \qquad f_{20}(\lambda) = a_{20}(\lambda) - \frac{a_{10}(\lambda)a_{11}(\lambda)}{a_{01}(\lambda)}, \qquad f_{11}(\lambda) = \frac{a_{11}(\lambda)}{a_{01}(\lambda)}, \\ &g_{00}(\lambda) = a_{00}(\lambda)a_{10}(\lambda), \qquad g_{10}(\lambda) = a_{01}(\lambda)b_{10}(\lambda) - a_{10}(\lambda)b_{01}(\lambda), \\ &g_{02}(\lambda) = \frac{b_{02}(\lambda)}{a_{01}(\lambda)}, \qquad g_{01}(\lambda) = a_{10}(\lambda) + b_{01}(\lambda), \\ &g_{11}(\lambda) = b_{11}(\lambda) + \frac{a_{10}(\lambda)a_{11}(\lambda)}{a_{01}(\lambda)} - \frac{2a_{10}(\lambda)b_{02}(\lambda)}{a_{01}(\lambda)}, \\ &g_{20}(\lambda) = a_{10}(\lambda)a_{20}(\lambda) + a_{01}(\lambda)b_{20}(\lambda) - a_{10}(\lambda)b_{11}(\lambda) \\ &\qquad - \frac{a_{10}^2(\lambda)a_{11}(\lambda)}{a_{01}(\lambda)} + \frac{a_{10}^2(\lambda)b_{02}(\lambda)}{a_{01}(\lambda)}. \end{aligned}$$

Next, applying the C^∞ transformation

$$u_2 = u_1, \qquad v_2 = f_{00}(\lambda) + v_1 + f_{20}(\lambda)u_1^2 + a_{11}(\lambda)u_1v_1 + \mathcal{O}\big(|u_1, v_1|^3\big),$$

system (9) becomes

$$\begin{aligned} \frac{\mathrm{d}u_2}{\mathrm{d}t} &= v_2, \\ \frac{\mathrm{d}v_2}{\mathrm{d}t} &= \alpha_{00}(\lambda) + \alpha_{10}(\lambda)u_2 + \alpha_{01}(\lambda)v_2 + \alpha_{20}(\lambda)u_2^2 \\ &\quad + \alpha_{11}(\lambda)u_2v_2 + \alpha_{02}(\lambda)v_2^2 + \mathcal{O}\big(|u_2, v_2|^3\big), \end{aligned} \tag{10}$$

where

$$\begin{aligned} \alpha_{00}(\lambda) &= g_{00}(\lambda) - f_{00}(\lambda)g_{01}(\lambda) - f_{00}^2(\lambda)f_{11}(\lambda) + f_{00}^2(\lambda) + f_{00}^2(\lambda)g_{02}(\lambda), \\ \alpha_{10}(\lambda) &= g_{10}(\lambda) - f_{00}(\lambda)g_{11}(\lambda) - f_{11}(\lambda)g_{00}(\lambda) - f_{00}(\lambda)f_{11}(\lambda)g_{01}(\lambda), \\ \alpha_{01}(\lambda) &= g_{01}(\lambda) - 2f_{00}(\lambda)g_{02}(\lambda) - f_{00}(\lambda)f_{11}(\lambda), \\ \alpha_{20}(\lambda) &= g_{20}(\lambda) + f_{11}(\lambda)g_{10}(\lambda) - f_{20}(\lambda)g_{01}(\lambda) - f_{00}(\lambda)f_{10}(\lambda)f_{11}(\lambda), \\ \alpha_{11}(\lambda) &= g_{11}(\lambda) + 2f_{20}(\lambda) - f_{00}(\lambda)f_{11}^2(\lambda), \\ \alpha_{02}(\lambda) &= g_{02}(\lambda) + f_{11}(\lambda) + f_{02}(\lambda)g_{01}(\lambda). \end{aligned}$$

Here $\alpha_{00}(0) = \alpha_{10}(0) = \alpha_{01}(0) = 0$, $\alpha_{20}(0) = g_{20}(0)$, $\alpha_{11}(0) = g_{11}(0) + 2f_{20}(0)$, and $\alpha_{02}(0) = f_{11}(0) + g_{02}(0)$.

In order to remove the term v_2 from the second equation of system (10), it is necessary to make the following substitutions. We assume that $\alpha_{11}(0) \neq 0$ and take the change

$$u_3 = u_2 + \frac{\alpha_{01}(\lambda)}{\alpha_{11}(\lambda)}, \qquad v_3 = v_2,$$

then system (10) is turned into

$$\begin{aligned}\frac{\mathrm{d}u_3}{\mathrm{d}t} &= v_3,\\ \frac{\mathrm{d}v_3}{\mathrm{d}t} &= \beta_{00}(\lambda) + \beta_{10}(\lambda)u_3 + \beta_{20}(\lambda)u_3^2\\ &\quad + \beta_{11}(\lambda)u_3v_3 + \beta_{02}(\lambda)v_3^2 + \mathcal{O}\bigl(|u_3, v_3|^3\bigr),\end{aligned} \tag{11}$$

where

$$\begin{aligned}\beta_{00}(\lambda) &= \alpha_{00}(\lambda) - \frac{\alpha_{10}(\lambda)\alpha_{01}(\lambda)}{\alpha_{11}(\lambda)} + \frac{\alpha_{20}(\lambda)\alpha_{01}^2(\lambda)}{\alpha_{11}^2(\lambda)},\\ \beta_{10}(\lambda) &= \alpha_{10}(\lambda) - \frac{2\alpha_{01}(\lambda)\alpha_{20}(\lambda)}{\alpha_{11}(\lambda)}, \qquad \beta_{20}(\lambda) = \alpha_{20}(\lambda),\\ \beta_{11}(\lambda) &= \alpha_{11}(\lambda), \qquad \beta_{02}(\lambda) = \alpha_{02}(\lambda).\end{aligned}$$

Now we take $u_4 = u_3$, $v_4 = v_3(1 - \beta_{02}u_3)$, and $\mathrm{d}t = (1 - \beta_{02}u_3)\,\mathrm{d}\tau$, still denote τ by t. Then system (11) is changed to

$$\begin{aligned}\frac{\mathrm{d}u_4}{\mathrm{d}t} &= v_4,\\ \frac{\mathrm{d}v_4}{\mathrm{d}t} &= \zeta_{00}(\lambda) + \zeta_{10}(\lambda)u_4 + \zeta_{20}(\lambda)u_4^2 + \zeta_{11}(\lambda)u_4v_4 + \mathcal{O}\bigl(|u_4, v_4|^3\bigr),\end{aligned} \tag{12}$$

where

$$\begin{aligned}\zeta_{00}(\lambda) &= \beta_{00}(\lambda), \qquad \zeta_{11}(\lambda) = \beta_{11}(\lambda),\\ \zeta_{20}(\lambda) &= \beta_{20}(\lambda) - 2\beta_{10}(\lambda)\beta_{02}(\lambda) + \beta_{02}^2(\lambda),\\ \zeta_{10}(\lambda) &= \beta_{10}(\lambda) - 2\beta_{00}(\lambda)\beta_{02}(\lambda).\end{aligned}$$

Finally, we take the scaling transformation

$$\sigma = \left|\frac{\zeta_{20}(\lambda)}{\zeta_{11}(\lambda)}\right|t, \qquad u_5 = \frac{\zeta_{11}^2(\lambda)}{\zeta_{20}(\lambda)}u_4, \qquad u_5 = \operatorname{sign}\biggl(\frac{\zeta_{11}(\lambda)}{\zeta_{20}(\lambda)}\biggr)\frac{\zeta_{11}^3(\lambda)}{\zeta_{20}^2(\lambda)}v_4.$$

Assume that $\zeta_{11}(0) = \alpha_{11}(0) \neq 0$, $\zeta_{20}(0) \neq 0$. Then system (12) turns into

$$\frac{\mathrm{d}u_5}{\mathrm{d}\sigma} = v_5, \qquad \frac{\mathrm{d}v_5}{\mathrm{d}\sigma} = \xi_1 + \xi_2u_5 + u_5^2 + \xi u_5v_5 + \mathcal{O}\bigl(|u_5, v_5|^3\bigr),$$

where

$$\xi_1 = \frac{\zeta_{00}(\lambda)\zeta_{11}^4(\lambda)}{\zeta_{20}^3(\lambda)}, \qquad \xi_2 = \frac{\zeta_{10}(\lambda)\zeta_{11}^2(\lambda)}{\zeta_{20}^2(\lambda)},$$

$$\xi = \operatorname{sign} \frac{\zeta_{11}(0)}{\zeta_{20}(0)} = \operatorname{sign} \frac{2f_{20}(0) + g_{11}(0)}{g_{20}(0)}$$

with the condition

$$\left| \frac{\partial(\xi_1, \xi_2)}{\partial(\lambda_1, \lambda_2)} \right|_{\lambda_{1,2}=0} = \begin{vmatrix} \frac{\partial \xi_1}{\partial \lambda_1} & \frac{\partial \xi_1}{\partial \lambda_2} \\ \frac{\partial \xi_2}{\partial \lambda_1} & \frac{\partial \xi_2}{\partial \lambda_2} \end{vmatrix}_{\lambda_{1,2}=0} \neq 0.$$

According to [11, Them. 8.4], we obtain the following theorem.

Theorem 8. *If the parameter satisfies the above nondegeneracy assumptions, then system* (2) *will exhibit the Bogdanov–Takens bifurcation at* E^*.

When $\xi = -1$, the following local bifurcation curve divides the neighborhood of the origin of the ξ_1, ξ_2-plane into four regions:

1. the saddle-node bifurcation curve $\mathrm{SN} = \{(\xi_1, \xi_2)\colon \xi_1 = \xi_2^2/4\}$;
2. the Hopf bifurcation curve $H = \{(\xi_1, \xi_2)\colon \xi_1 = 0,\ \xi_2 < 0\}$;
3. the homoclinic bifurcation curve $\mathrm{HL} = \{(\xi_1, \xi_2)\colon \xi_1 = -6\xi_2^2/25 + o(\xi_2^2),\ \xi_2 < 0\}$.

Remark 1. If $c_0 = b + 2e + 1 - 2\sqrt{be + e^2 + b + e}$, we also have $\Delta = 0$, and system (2) will admit the Bogdanov–Takens bifurcation at E^*. Analysis is similar to the above.

Remark 2. When $\xi = +1$, the system has similar local bifurcation curves. In this case, the system can be changed as the above by $t \mapsto -t$ and $\xi_2 \mapsto -\xi_2$.

4 Numerical simulations

In this section, we validate the results of the preceding analysis through numerical simulations. The parameters of the system, denoted as a, b, c, d, and e, are utilized in the simulations. Numerical simulations and phase portraits have been carried out by using MATLAB with fixed parameters and varying conditions.

Example 1. In Fig. 1(a), the dynamics of system (2) are displayed with $a = 1$, $b = 0.2$, $c = 0.25$, $d = 7.5$. The system always has four boundary equilibria: two saddle-points $E_0 = (0, 0)$ and $E_3 = (1, 0)$, a stable node E_1, and a unstable node $E_2 = (0.2, 0)$. In this case, $e_{\mathrm{SN}} = ((b + 1 - c/a)^2 a - 4ab)/(4c) = 0.1025$. In the left panel of Fig. 1(a), $e = 0.2 > e_{\mathrm{SN}}$, the system does not have any positive equilibria. In the middle of Fig. 1(a), $e = e_{\mathrm{SN}}$, the system has a unique positive equilibrium point $E^* = (0.475, 0.5775)$, and saddle-node bifurcation may occur near E^*. In the diagram on the right in Fig. 1(a), $e = 0.09 < e_{\mathrm{SN}}$, the system has two distinct positive equilibria $E_4 = (0.4191, 0.5091)$ and $E_5 = (0.5309, 0.6209)$.

Example 2. Figure 1(b) shows the dynamical behaviors of system (2) with $a = 1$, $b = 0.15$, $c = 0.36$, $e = 0.0167$. The system has four boundary equilibria: two saddle-points $E_0 = (0, 0), E_3 = (1, 0)$, a stable node $E_1 = (0, 0.0167)$, and a unstable node $E_2 = (0.15, 0)$. Here $d_0 = 2a/((ab + a - c)c) - a(b - 1)^2)/(4c) + c/(4a) = 6.6206$. In

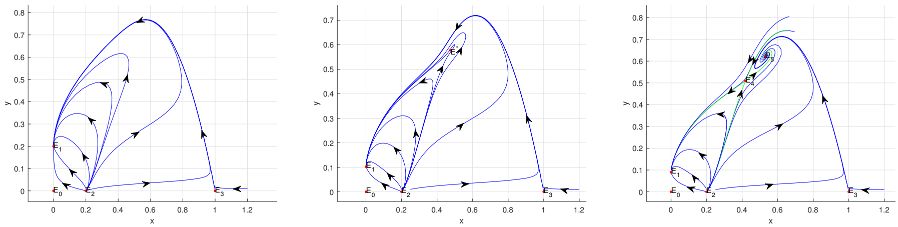

(a) $a = 1$, $b = 0.2$, $c = 0.25$, $d = 7.5$

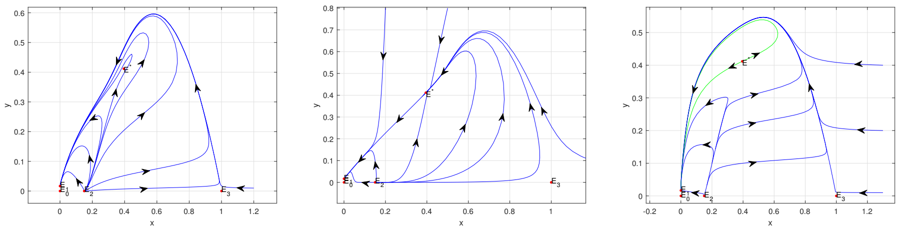

(b) $a = 1$, $b = 0.15$, $c = 0.36$, $e = 0.0167$

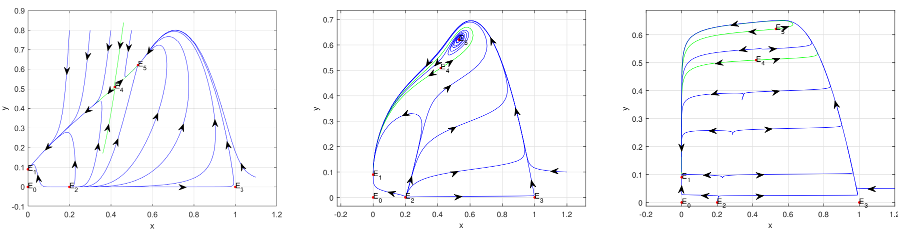

(c) $a = 1$, $b = 0.2$, $c = 0.25$, $e = 0.09$

Figure 1. Dynamics of system (2).

the left panel of Fig. 1(b), $d = d_0 = 6.6206$, the system has a unique positive equilibrium $E^* = (0.3950, 0.4117)$, which is a cusp of codimension 2, so the system undergoes the Bogdanov–Takens bifurcation around E^*. In the middle of Fig. 1(b), $d = 1 < d_0$, the unique positive equilibrium E^* is an attracting saddle-node. In the diagram on the right in Fig. 1(b), $d = 30 > d_0$, the unique positive equilibrium E^* is a repelling saddle-node.

Example 3. In Fig. 1(c), the dynamics of system (2) are presented with $a = 1$, $b = 0.2$, $c = 0.25$, $e = 0.09$. Similar to Fig. 1(b), the system has four boundary equilibria: two saddle-points $E_0 = (0, 0)$, $E_3 = (1, 0)$, a stable node $E_1 = (0, 0.09)$, and a unstable node $E_2 = (0.2, 0)$. Meanwhile, the system have two distinct positive equilibria $E_4 = (x_4, y_4) = (0.4191, 0.5091)$, $E_5 = (x_5, y_5) = (0.5309, 0.6209)$. In addition, we have $d_{\mathrm{H}} = 1/([-3x_5^2 + 2(b + 1)x_5 - b]a - cy_5) - y_5 = 13.0089$. In the picture on the left side of Fig. 1(c), $d = 0.99 < d_{\mathrm{H}}$, E_5 is a stable node. In the middle picture of Fig. 1(c), $d = d_{\mathrm{H}}$, E_5 is a linear center. In the picture on the right side of Fig. 1(c), $d = 200 > d_{\mathrm{H}}$, E_5 is a unstable node. So the Hopf bifurcation may happen near E_5.

Example 4. In the picture on the left side of Fig. 2, the dynamics of system (2) are presented with $a = 1$, $b = 0.2$, $c = 0.025$, $d = 7.5$. In the rest of the figures in Figs. 2–4, the dynamics of system (2) are exhibited with $a = 1$, $b = 0.15$, $c = 0.36$, $d = 6.620614$, $e = 0.016736$. The critical values of bifurcation parameters are c_0 and d_0. By calculation, we get $\alpha_{11}(0) = -0.4097792 \neq 0$, $\zeta_{20}(0) = -0.0561689 \neq 0$, and

$$\left|\frac{\partial(\xi_1, \xi_2)}{\partial(\lambda_1, \lambda_2)}\right| = -1.085704 \neq 0.$$

So from Theorem 8, in this case, system (2) will experience the Bogdanov–Takens bifurcation at E^*. Moreover, for small λ_i ($i = 1, 2$), the bifurcation curves can be locally approximated as

$$\begin{aligned}
\mathrm{SN} &= \bigl\{(\lambda_1, \lambda_2)\colon\ \lambda_1 = 0,\ \lambda_2 \neq 0\bigr\};\\
\mathrm{H} &= \bigl\{(\lambda_1, \lambda_2)\colon\ 350.4886\lambda_1^2 + 14.2278\lambda_1\lambda_2 + 3.6798\lambda_1 + 0.0218\lambda_2^2 = 0,\ \lambda_2 > 0\bigr\};\\
\mathrm{HL} &= \bigl\{(\lambda_1, \lambda_2)\colon\ 356.3012\lambda_1^2 + 14.9247\lambda_1\lambda_2 + 3.6798\lambda_1 + 0.0427\lambda_2^2 = 0,\ \lambda_2 > 0\bigr\}.
\end{aligned}$$

Figures 2–4 show the subcritical Bogdanov–Takens bifurcation diagram and phase portraits of system (2).

(a) In the left panel of Fig. 2, it is shown that the number of equilibrium points of the system changes as the parameter e varies, where a saddle-node bifurcation occurs near the LP point, and a Hopf bifurcation occurs near the H point

(b) In the middle panel of Fig. 2, the bifurcation curves SN, H, and HL divide the λ_1, λ_2-plane into four regions, rotating counterclockwise around the critical parameter value of the Bogdanov–Takens bifurcation $(\lambda_1, \lambda_2) = (0, 0)$.

(c) When the parameter lies in the region I, then system (2) has no positive point of equilibrium (as in the right panel of Fig. 2).

(d) When the parameter is situated on the curve SN, a unique positive equilibrium point E^*, i.e., a saddle-node, will emerge.

(e) When the parameter crosses the curves SN and enters region II, the system undergoes a saddle-node bifurcation, resulting in the emergence of two positive equilibrium points E_4 and E_5. One of these equilibrium points is a saddle-point, while the other is an unstable focus (as in the left panel of Fig. 3).

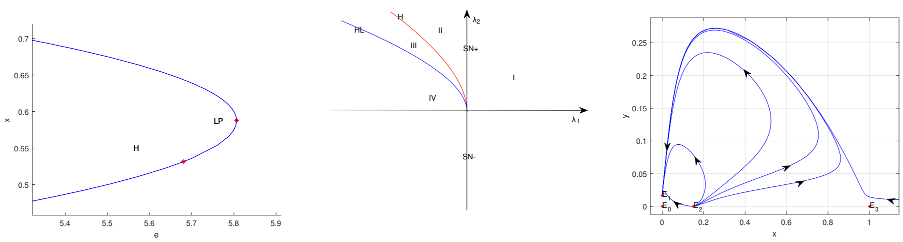

Figure 2. The panels are the saddle-node branching diagram, the Bogdanov–Takens bifurcation diagram, and the bottom one shows no equilibria when $(\lambda_1, \lambda_2) = (1, 0.005)$ is in region I.

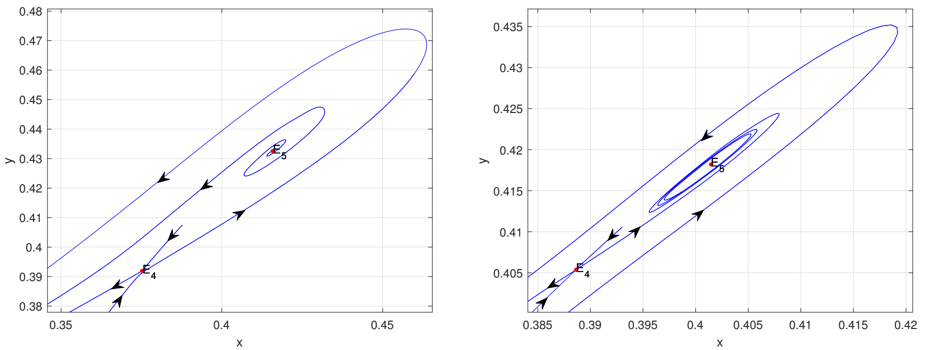

Figure 3. The left panel represents the unstable focus when $(\lambda_1, \lambda_2) = (-0.001, 2)$ lies in region II, and the right panel presents the unstable limit cycle when $(\lambda_1, \lambda_2) = (-0.0001, 0.05)$ is in region III.

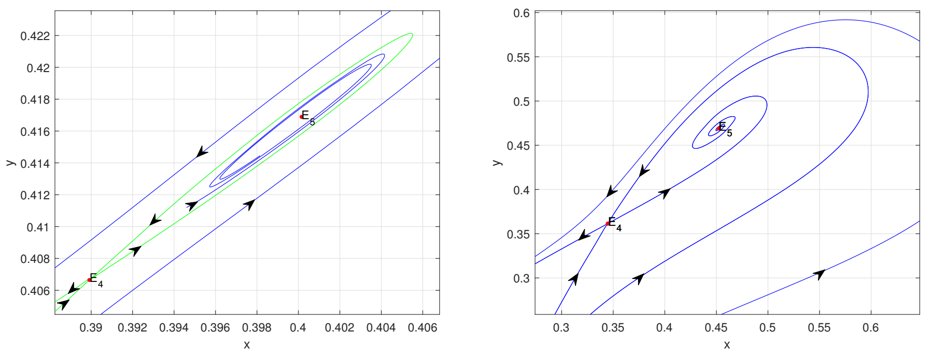

Figure 4. The left panel describes an unstable homoclinic cycle when $(\lambda_1, \lambda_2) = (-0.00006367, 0.06453)$ is on the curve HL, and the right panel represents a stable focus when $(\lambda_1, \lambda_2) = (-0.007, -0.01)$ is in region IV.

(f) When the parameter is situated on the curve H, system (2) exhibits two positive equilibrium points. One is an unstable weak focus, while the other is a saddle-point.

(g) When the parameter crosses the curve H and enters the region III through the subcritical Hopf bifurcation, an unstable cycle emerges, where the focus remains stable (as in the right panel of Fig. 3).

(h) When the parameter goes on changing until it lies on the curve HL, passing through the homoclinic bifurcation, an unstable homoclinic orbit containing a stable focus appears (as in the left panel of Fig. 4).

5 Conclusion

In view of the Allee effect on prey and fear effect on predator, the modified Leslie–Gower predator–prey system exhibits complex dynamics. The model can have some degenerate points, such as the saddle-node point, the fine focus, and the cusp point of codimension 2, in addition to some hyperbolic points. Under parameter perturbation, the system can experience different and interesting bifurcations, such as the saddle-node bifurcation, the Hopf bifurcation, and the Bogdanov–Takens bifurcation of codimension 2. As a result of these bifurcations, the equilibrium point, the periodic cycle, and the homoclinic orbit will appear in the system. From the findings the predators and prey could coexist in the long run or coexist periodically, and that may be helpful to understand interaction between them. In particular, when predators have alternative prey, it facilitates the coexistence of predators and prey. From the results we find that predator and prey populations can have long-term stable coexistence or the cyclical coexistence status. That implies the strong Allee effect on the prey population, as well as the fear-influenced predators' behaviors, have clear implications for the stability and the persistence of population interactions. Particularly, if the density of prey population is close to the Allee threshold, the dynamics may become highly sensitive, and ecosystems become more susceptible to external disturbances. From an ecological point of view, the results offer some theoretical basis to discover the complex dynamics in predator–prey systems, especially, when the vulnerable prey population need to be protected and predation numbers should be managed. These can also explain the observed phenomena in similar systems in practice and offer potential instruction to develop conservation and management strategies.

Author contributions. All authors (R.W. and W.X.) have contributed as follows: methodology, formal analysis, validation, writing – review and editing, R.W.; software, writing – original draft preparation, W.X. All authors have read and approved the published version of the manuscript.

Conflicts of interest. The authors declare no conflicts of interest.

References

1. W. Allee, *Animal Aggregations: A Study in General Sociology*, Univ. Chicago Press, Chicago, 1931, https://doi.org/10.5962/bhl.title.7313.
2. M.A. Aziz-Alaoui, M.D. Okiye, Boundedness and global stability for a predator-prey model with modified Leslie-Gower and Holling-type II schemes, *Appl. Math. Lett.*, **16**(7):1069–1075, 2003, https://doi.org/10.1016/S0893-9659(03)90096-6.
3. L. Berec, E. Angulo, F. Courchamp, Multiple Allee effects and population management, *Trends Ecol. Evol.*, **22**(4):185–191, 2007, https://doi.org/10.1016/j.tree.2006.12.002.
4. S. Creel, D. Christianson, Relationships between direct predation and risk effects, *Trends Ecol. Evol.*, **23**(4):194–201, 2008, https://doi.org/10.1016/j.tree.2007.12.004.
5. A. Das, G.P. Samanta, A prey–predator model with refuge for prey and additional food for predator in a fluctuating environment, *Physica A*, **538**:122844, 2020, https://doi.org/10.1016/j.physa.2019.122844.
6. B. Dennis, Allee effects: population growth, critical density, and the chance of extinction, *Nat. Resour. Model.*, **3**(4):481–538, 1989, https://doi.org/10.1111/j.1939-7445.1989.tb00119.x.

7. S. Eggers, M. Griesser, M. Nystrand, J. Ekman, Predation risk induces changes in nest-site selection and clutch size in the Siberian jay, *Proc. R. Soc. B-Biol. Sci.*, **273**(1587):701–706, 2006, https://doi.org/10.1098/rspb.2005.3373.
8. Q. Fang, X. Li, Complex dynamics of a discrete predator–prey system with a strong Allee effect on the prey and a ratio-dependent functional response, *Adv. Difference Equ.*, **1**:320, 2018, https://doi.org/10.1186/s13662-018-1781-x.
9. E. González-Olivares, A. Rojas-Palma, B. González-Ya nez, Multiple limit cycles in a Leslie–Gower-type predator–prey model considering weak Allee effect on prey, *Nonlinear Anal. Model. Control*, **22**(3):347–365, 2017, https://doi.org/10.15388/NA.2017.3.5.
10. A.M. Kramer, B. Dennis, A.M. Liebhold, J.M. Drake, The evidence for Allee effects, *Popul. Ecol.*, **51**(3):341–354, 2009, https://doi.org/10.1007/s10144-009-0152-6.
11. Y.A. Kuznetsov, *Elements of Applied Bifurcation Theory*, Springer, New York, 1995, https://doi.org/10.1007/978-3-031-22007-4.
12. P.H. Leslie, J.C. Gower, The properties of a stochastic model for the predator-prey type of interaction between two species, *Biometrika*, **47**(3-4):219–234, 1960, https://doi.org/10.1093/biomet/47.3-4.219.
13. T. Liu, L. Chen, F. Chen, Z. Li, Dynamics of a Leslie–Gower model with weak Allee effect on prey and fear effect on predator, *Int. J. Bifurcation Chaos*, **33**(1):2350008, 2023, https://doi.org/10.1142/S0218127423500086.
14. M.A. Mccarthy, The Allee effect, finding mates and theoretical models, *Ecol. Model.*, **103**:99–102, 1997, https://doi.org/10.1016/S0304-3800(97)00104-X.
15. P. Panday, N. Pal, S. Samanta, J. Chattopadhyay, A three species food chain model with fear induced trophic cascade, *Int. J. Appl. Comput. Math.*, **5**:100, 2019, https://doi.org/10.1007/s40819-019-0688-x.
16. L. Perko, *Differential Equations and Dynamical Systems*, Springer, New York, 2001, https://doi.org/10.1007/978-1-4613-0003-8.
17. R.M. Pringle et al., Predator-induced collapse of niche structure and species coexistence, *Nature*, **570**:58–64, 2019, https://doi.org/10.1038/s41586-019-1264-6.
18. L. Puchuri, O. Bueno, E. Gonzlez-Olivares, A. Rojas-Palma, Simultaneous Hopf and Bogdanov–Takens bifurcations on a Leslie–Gower type model with generalist predator and group defense, *Qual. Theory Dyn. Syst.*, **23**:255, 2024, https://doi.org/10.1007/s12346-024-01118-5.
19. N. Sarif, S. Sarwardi, Complex dynamical study of a delayed prey–predator model with fear in prey and square root harvesting of both species, *Chaos*, **33**(3):033112, 2023, https://doi.org/10.1063/5.0135181.
20. J.P. Suraci, M. Clinchy, L.M. Dill, D. Roberts, L.Y. Zanette, Fear of large carnivores causes a trophic cascade, *Nat. Commun.*, **7**(1):10698, 2016, https://doi.org/10.1038/ncomms10698.
21. V. Volterra, Fluctuations in the abundance of a species considered mathematically, *Nature*, **118**: 558–560, 1926, https://doi.org/10.1038/118558a0.
22. X. Wang, L. Zanette, X. Zou, Modelling the fear effect in predator–prey interactions, *J. Math. Biol.*, **73**(5):1179–1204, 2016, https://doi.org/10.1007/s00285-016-0989-1.

23. S. Wiggins, *Introduction to Applied Nonlinear Dynamical Systems and Chaos*, Springer, New York, 2003, https://doi.org/10.1007/b97481.

24. D. Wu, H. Zhao, Y. Yuan, Complex dynamics of a diffusive predator–prey model with strong Allee effect and threshold harvesting, *J. Math. Anal. Appl.*, **469**(2):982–1014, 2019, https://doi.org/10.1016/j.jmaa.2018.09.047.

25. C. Xiang, J. Huang, S. Ruan, D. Xiao, Bifurcation analysis in a host-generalist parasitoid model with Holling II functional response, *J. Differ. Equations*, **268**(8):4618–4662, 2020, https://doi.org/10.1016/j.jde.2019.10.036.

26. D. Xiao, S. Ruan, Bogdanov-Takens bifurcations in predator-prey systems with constant rate harvesting, in S. Ruan, G.S.K. ail S. K. Wolkowicz, J. Wu (Eds.), *Differential Equations with Applications to Biology. Proceedings of the International Conference, Halifax, Canada, July 25–29, 1997*, Fields Inst. Commun., Vol. 21, AMS, Providence, RI, 1999, pp. 493–506.

27. F. Zhang, Y. Chen, J. Li, Dynamical analysis of a stage-structured predator-prey model with cannibalism, *Math. Biosci.*, **307**:33–41, 2019, https://doi.org/10.1016/j.mbs.2018.11.004.